Modern Laser Scanning Confocal Microscopy

Peter O. Bayguinov,[1] Dennis M. Oakley,[1] Chien-Cheng Shih,[1] Daniel J. Geanon,[1] Matthew S. Joens,[1] and James A. J. Fitzpatrick[1,2,3,4]

[1]Center for Cellular Imaging, Washington University in St. Louis, St. Louis, Missouri
[2]Departments of Cell Biology & Physiology and Neuroscience, Washington University School of Medicine, St. Louis, Missouri
[3]Department of Biomedical Engineering, Washington University in St. Louis, St. Louis, Missouri
[4]Corresponding author: *fitzp@wustl.edu*

Since its commercialization in the late 1980's, confocal laser scanning microscopy (CLSM) has since become one of the most prevalent fluorescence microscopy techniques for three-dimensional structural studies of biological cells and tissues. The flexibility of the approach has enabled its application in a diverse array of studies, from the fast imaging of dynamic processes in living cells, to meticulous morphological analyses of tissues, and co-localization of protein expression patterns. In this chapter, we introduce the principles of confocal microscopy and discuss how the approach has become a mainstay in the biological sciences. We describe the components of a CLSM system and assess how modern implementations of the approach have further expanded the use of the technique. Finally, we briefly outline some practical considerations to take into account when acquiring data using a CLSM system.

Keywords: confocal laser scanning microscopy (CLSM) • fluorescent imaging • live-cell imaging • optical sectioning • spinning disk confocal • swept-field confocal • three-dimensional imaging

How to cite this article:
Bayguinov, P. O., Oakley, D. M., Shih, C.-C., Geanon, D. J., Joens, M. S., & Fitzpatrick, J. A. J. (2018). Modern laser scanning confocal microscopy. *Current Protocols in Cytometry*, *85*, e39. doi: 10.1002/cpcy.39

INTRODUCTION

The use of fluorescent reporter probes has become ubiquitous in the study of the three-dimensional structure and dynamic behavior of biological systems (Pawley, 2006). Their use stems from analyses of protein co-localization (Dunn, Kamocka, & McDonald, 2011), assessment of the three-dimensional morphology of a specimen (Wallén et al., 1991), the study of dynamic processes such as calcium signaling (Roe, Fiekers, Philipson, & Bindokas, 2006; Scheenen & Carmignoto, 2002), and single molecule diffusion (Osborne, Balasubramanian, Furey, & Klenerman, 1998; Vukojevic et al., 2008). Coincident with the proliferation in the application of fluorescence detection methods has been the need for more sensitive microscopy approaches capable of higher resolution, gentler imaging, and faster acquisition rates. To that end, confocal laser scanning microscopy, with its varying permutations, has become an indispensable imaging tool to any study utilizing fluorescent probes. Before we delve into the principles behind the technique, it is important to understand why the development of confocal microscopy was a necessity.

Current Protocols in Cytometry e39, Volume 85
Published in Wiley Online Library (wileyonlinelibrary.com).
doi: 10.1002/cpcy.39

The overarching goal of any microscopy approach is to generate contrast between a sample and its background. In fluorescent imaging, this contrast can be defined as the difference between the signal originating from the focal plane, and the out-of-focus fluorescence. Epi-fluorescent imaging alone can generate great resolution and sensitivity in samples that are relatively thin (typically ~5 μm or thinner). In thicker samples, light scattering from above and below the focal plane begin to interfere with the acquisition of the primary signal. As a result, over the last several decades, there have been a number of novel approaches developed to facilitate optical sectioning which are aimed at improving fluorescence contrast by reducing the effects of scattered light. These include the development of multiphoton microscopy (Denk, Strickler, & Webb, 1990), structured illumination optical sectioning (Neil, Juskaitis, & Wilson, 1997; Wilson, 2011), total internal reflection fluorescence (TIRF) microscopy (Axelrod, 1981), as well as the development and application of computational post-processing approaches, such as deconvolution (Erhardt, Zinser, Komitowski, & Bille, 1985). Nonetheless, during this time span, the most readily adopted fluorescent microscopy technique has been confocal laser scanning microscopy (CLSM; Brakenhoff, van Spronsen, van der Voort, & Nanninga, 1989; White, Amos, & Fordham, 1987). The primary appeal of CLSM is its versatility. The method is well-suited to studying morphological features, recording dynamics in living cells, and can be readily integrated with other imaging modes, such as spectral imaging (Dickinson, Bearman, Tille, Lansford, & Fraser, 2001; Haraguchi, Shimi, Koujin, Hashiguchi, & Hiraoka, 2002) and FRET (Sekar & Periasamy, 2003).

In this chapter, we will discuss the principles that underlie confocal microscopy, the essential components of a confocal microscope, and how new developments in those technologies have allowed for an expansion of the technique. We will describe some of the variations on the technique, particularly spinning disk and swept field confocal systems, as well as some of the limitations associated with each approach. Finally, we will explore some of the practical considerations when using CLSM, many of which are broadly applicable to all microscopic-based imaging approaches.

PRINCIPLES AND DEVELOPMENT OF CONFOCAL MICROSCOPY

The term *confocal* defines objects that have a conjugate focal plane. In microscopy, this refers to the coincidence between the focal plane of the objective lens and the detector, whereby the in-focus image plane is isolated from adjacent axial planes. The defining feature of confocal microscopy is the use of a diffraction-limited spot of light to illuminate the sample and an aperture (or pinhole) in the collection light path at conjugate focus with this spot to generate such isolation (or optical sectioning).

A Historical Perspective

The first confocal microscope was designed by Marvin Minsky in 1955 while he was a Junior Fellow at Harvard (Minsky, 1957; Minsky, 1988). In his attempts to image connections among interneurons, Minsky realized he could achieve significant resolution improvements by illuminating only a small section of a sample and scan across it in a point-by point manner, thereby reducing the magnitude of light scattering. To realize this, he made use of a pinhole situated in front of an arc lamp, effectively reducing the spread of the excitation light field to a diffraction- limited spot on the sample. To reduce the light scattering within the column of excitation, Minsky introduced a second pinhole in front of the detector, which served to reject light that originated from outside of the focal plane. Images were captured using a low noise photomultiplier with image data output on an old radar screen. The final microscope that was developed (see schematic in Fig. 1A) allowed for the scanning of larger samples by moving them in a rectangular raster pattern.

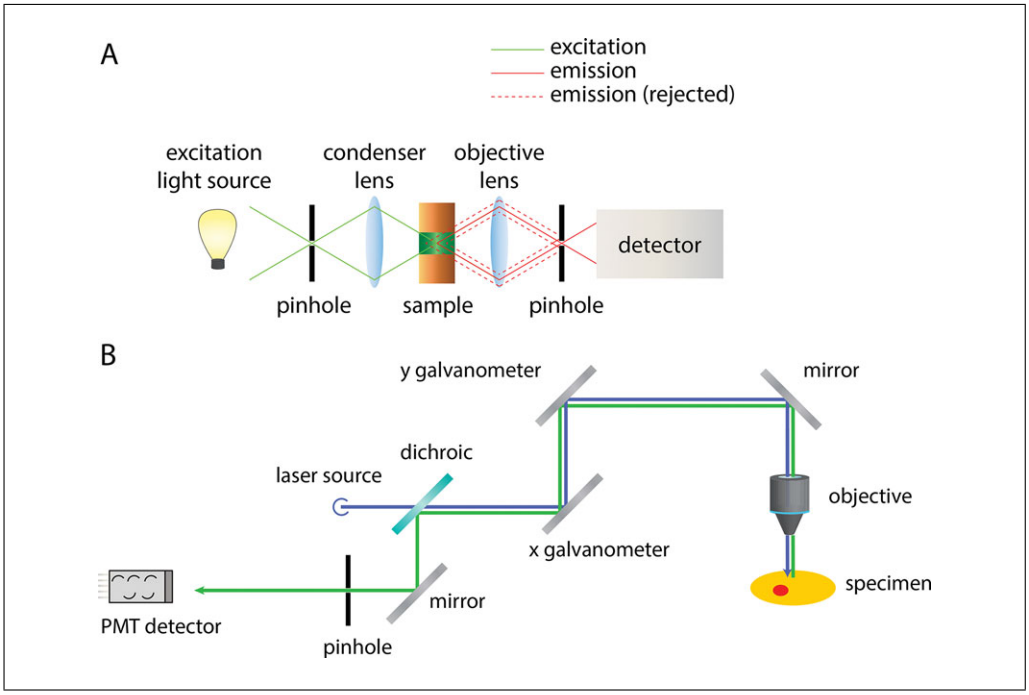

Figure 1 Design of the confocal microscope. (**A**) Minsky's original transmission confocal microscope. Image adopted from Minsky (1988). The excitation light source (green line) is collimated by the first pinhole, and is then focused onto the specimen by the condenser lens. The emission light at the focal point is focused through the objective and through the second pinhole to the detector (red line), while out of focus light is rejected at the pinhole (dotted red line). (**B**) A schematic representation of a modern confocal laser scanning microscope. Excitation light, emitted from a laser source is passed through a dichroic mirror, and is scanned across the field of view on the specimen by a pair of galvanometers, which scan in the x and y axes. Emitted light is reflected back via the galvanometers to the dichroic where it is reflected through the pinhole to a PMT detector.

In spite of the potential advantages the confocal microscope offered, there were only a few adaptations or improvements in the intervening decades on Minsky's original design (Brakenhoff, Blom, & Barends, 1979; Davidovits & Egger, 1969). There are several reasons as to why this approach did not receive wider adoption. For one, the confocal approach required technologies which were either underdeveloped or non-existent at the time. Lasers, which provide a coherent light source that could be readily used for confocal microscopy, were only developed in the early 1960's (Bridges, 1964; Maiman, 1960; White & Ridgen, 1962). Likewise, computers necessary for image digitalization, and photomultiplier tubes optimized for high-efficiency detection were only just emerging. In an interview some years later, Minsky himself admitted that he made mistakes in the way the resultant confocal images were presented on his original microscope, and that a more attractive way of displaying them might have sparked more interest. Nonetheless, the most probable reason as to why the confocal microscope was not adopted and developed further at that time was that there was no pressing need for it by the scientific community.

Whilst fluorescently tagged antibodies were developed in the early 1940's, the fundamental realization that they could be used to label different proteins of interest did not occur until the 1970's (Julius, Masuda, & Herzenberg, 1972; Lazarides & Weber, 1974). This led to a dramatic increase in interest in the use of fluorescence microscopy to study various immuno-histochemical targets. But, with the concomitant increase in epi-fluorescence imaging, it became quickly apparent that the imaging of thick tissue sections was largely limited by effects of light scattering. As a number of researchers altered their scientific approaches by imaging cultured cell monolayers, or by flattening their samples, several

groups sought to develop a fluorescent microscope capable of imaging thicker samples with high fidelity.

The modern, and first commercially-successful confocal laser scanning microscope was developed by Brad Amos and John White at the University of Cambridge (Amos, White, & Fordham, 1987; White et al., 1987). Their design incorporated a number of fundamental changes, which allowed the instrument to rapidly scan thick biological samples with minimal perturbation during scans. The light source they chose was an Argon ion laser which they scanned across the field of view of the imaging objective through the use of two scanning galvanometers (one each for the x and y directions of scanning). This method of scanning the light beam rather than moving the specimen, was based on the 'flying spot' microscope conceptualized in the 1950's (Young & Roberts, 1951), and presented significant improvements in vibration reduction, accuracy, and speed, when compared to moving stage designs. The resultant image was collected by the same galvanometers, and projected onto an adjustable aperture to allow for optimized pinhole size for different fluorophores, and was recorded by a PMT onto a computer using a frame store card (Fig. 1B; Amos & White, 2003). This design was marketed by BioRad as the MRC 500, and it served as the basis for all modern CLSM systems.

Resolution Advantages of Confocal Microscopy

In fluorescent microscopy, the intensity of light emitted from a single point is described by a point spread function (PSF), having an increased probability at the center, and a decreased probability towards the periphery. This PSF has the appearance of a disk with concentric rings of decreasing intensity, a pattern known as an Airy disk (Fig. 2A). The resolving power of a fluorescent system is described by the width of the Airy disk, which is dependent on the numerical aperture of the objective and the excitation wavelength used, per the Abbe equation:

$$d = \frac{\lambda}{2n \sin\theta} = \frac{\lambda}{2\mathrm{NA}}$$

where λ represents the excitation wavelength of light and NA is the numerical aperture of a lens.

Another useful measurement of resolution is the point where intensity falls to 50% of the peak, the full width half maximum (FWHM; Fig. 2A). At this point we can calculate the lateral resolution for widefield fluorescent imaging as:

$$\mathrm{FWHM}_{\mathrm{lateral}} = \frac{0.51\lambda}{\mathrm{NA}}$$

and the lateral resolution of a confocal image with an infinitely-small aperture as:

$$\mathrm{FWHM}_{\mathrm{lateral}} = \frac{0.37\lambda}{\mathrm{NA}}$$

This effectively suggests that in the lateral plane, confocal microscopy offers a theoretical maximum resolution improvement of $\sqrt{2}$ (Wilson, 2011).

The point spread function applies not only to the horizontal focal plane, but also to the axial (vertical) plane. Plotting this spread along the z-axis (Fig. 2B) shows the conical

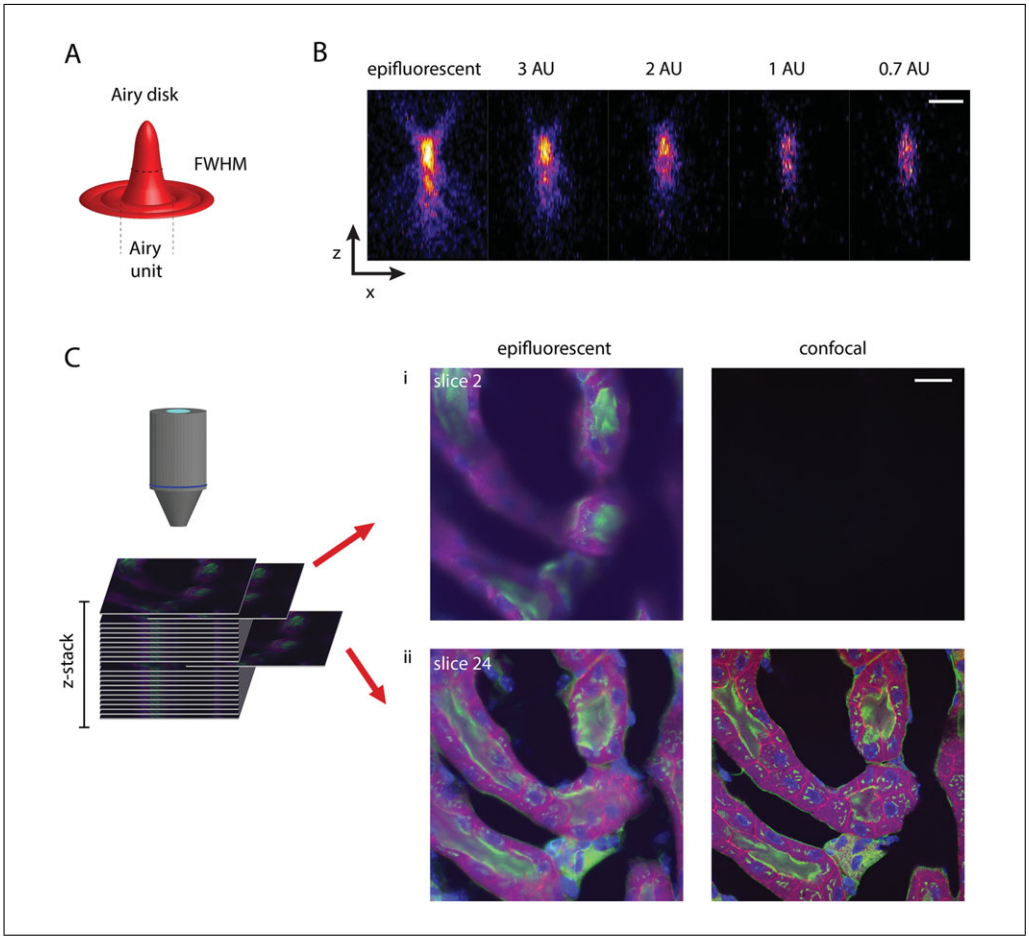

Figure 2 Resolution advantages of the confocal microscope. (**A**) Three-dimensional rendering of an Airy disk. Note the demarcations for an Airy unit and the full-width half-maximum point. (**B**) The axial point spread function of a 200 μm fluorescent bead, shown under epifluorescent illumination with a confocal aperture of 3, 2,1 and 0.7 Airy units. Scale bar = 1 μm. (**C**) Side by side comparison of multidimensional epifluorescent and confocal microscopy of the same thick sample. The three-dimensional stack of images is a visual representation of the optical sectioning performed with both techniques. Note the difference in scattered light recorded by each approach at the top of the stack (i). The decreased out-of-focus fluorescence is directly attributable to the increases in contrast and resolution in the confocal image from the middle of the stack (ii). Fixed mouse kidney section, Alexa Fluor 488 wheat germ agglutinin, Alexa Fluor 568 phalloidin, and DAPI. Scale bar = 20 μm.

spread of fluorescence above and below the fluorescent object. The FWHM for this function is described as:

$$\mathrm{FWHM}_{\text{axial WF}} = \frac{0.89\lambda}{n - \sqrt{n^2 - NA^2}} \text{ and } \mathrm{FWHM}_{\text{axial CONFOCAL}} = \frac{0.64\lambda}{n - \sqrt{n^2 - NA^2}}$$

The maximal axial resolution gains that confocal microscopy offers are ~1.4 fold, and this gain is a function of the confocal aperture. This can be seen in Figure 2B, where reducing the confocal pinhole from 3 to 2 to 1 to 0.7 Airy units incrementally decreases the lateral spread of the function. Of particular note is the term 'Airy unit', which is used to describe the size of the confocal aperture. As an Airy unit (the diameter of the central spot, Fig. 2A) is defined by both the wavelength of the excitation light and the numerical aperture of a given lens, each fluorophore/objective combination yields a different diameter value for an Airy unit. We will return to this topic in the Practical Considerations section below.

The resolution advantages of confocal microscopy are immediately apparent in images when one compares them side by side with epifluorescent acquisitions of biological tissues thicker than a few micrometers. Taking a series of images at different focal planes, thus generating what is routinely referred to as a 'z-stack' (as illustrated in Fig. 2C), shows the resolution and contrast gains offered by confocal microscopy as well as the underlying reason for those gains. Examining images from the top of the stack (Fig. 2Ci), where the imaging plane is above the tissue, shows scattered light spreading in the epifluorescent image, while the confocal image appears black. This reduction in the axial PSF directly results in the differences in resolving power observed in optical sections from the middle of the z-stack (Fig. 2Cii).

COMPONENTS OF A CONFOCAL LASER SCANNING MICROSCOPE

The principles that underlie a CLSM are fairly simple, but can be implemented in a fairly complex manner. As fluorescent imaging is a linear imaging technique, we will assume the confocal microscope is the sum of its parts, and discuss each component, along with some of the modern alternatives that have emerged.

Detectors

Most modern CLSM systems with a point source capture approach utilize a photomultiplier tube (PMT) to capture emitted photons that result from the process of fluorescence. A PMT has a light-sensitive photocathode which converts captured photons into photoelectrons, which are then amplified via a series of dynodes. This allows the signal to be digitized through an analogue-to-digital converter, and thus be acquired by software as a grayscale value at a desired bit-depth. Traditionally, PMTs have a fairly poor quantum efficiency, on the order of ~20%, but have become mainstays in fluorescent microscopy due to their low signal to noise and their high dynamic range.

Over the past 15 years there have been a number of advances in the design of PMTs, substantially increasing both their quantum efficiency and sensitivity. Use of gallium arsenide phosphide (GaAsP) as a photocathode material has increased the quantum efficiency up to 42%, which is tantalizingly close to the theoretical limit of 50% for such devices (Zipfel, Williams, & Webb, 2003). The GaAsP detectors offer excellent efficiency in the 400 to 650 nm range, but their sensitivity drops off dramatically beyond that, requiring them to be used in conjunction with traditional PMTs for detection of both UV and far-red fluorescence.

In contrast, certain semiconductor devices, such as the avalanche photodiode (APD), have been combined with photocathodes to generate a range of hybrid detectors. Such devices offer an order of magnitude increase in amplification, when compared with PMTs, thus making them particularly suitable for low-fluorescence detection paradigms. This sensitivity comes at a price, and these hybrid detectors have been shown to generate significantly more dark current, in many cases nullifying the signal-to-noise gains that their increased sensitivity offers (Stokes, 2005).

The geometrical nature of detectors has evolved drastically in recent years to allow for the simultaneous capture of the emission spectra of multiple fluorophores. Traditionally, separate PMT detectors were used in conjunction with dichroic mirrors and bandpass emission filters, allowing for the detection of emission from individual fluorophores labels. Spectral array detectors have now become commonplace, allowing for the simultaneous detection of the entire emission spectrum. This approach uses a diffraction grating to spectrally disperse the emitted light, and then project it across a multi-anode PMT. These PMTs, typically GaAsP-based, are capable of recording the entire visible spectrum with <10 nm resolution. There are a number of advantages that arise from the

use of spectral detectors. Spectral imaging uses the detection array to record the emission of a fluorophore throughout the entire visible region of the electromagnetic spectrum, thus generating what is termed a 'λ-stack.' Such stacks can be extremely useful for assessing the optimal emission of a sample, thus allowing the user to optimize acquisition settings and thus improve the signal to noise ratio in their acquired image data. Array detectors are also invaluable in spectral unmixing, or the separation of two or more overlapping emission spectra, thus permitting the use of fluorescent labels which would otherwise produce crosstalk when imaged using the traditional approach of dichroic mirror and bandpass filter imaging. Lastly, the integration of spectral array detectors in CLSM systems enables the use of novel probes with unique emission characteristics without the need for further equipment upgrades. One downside to spectral array PMTs however is their increased cost, and that they require meticulous calibration for optimal performance (Cole et al., 2013).

Spatial Light Modulators

The means by which excitation light is scanned, and fluorescence emission is collected across an image, is essential in determining the precision, speed, and signal to noise attributes of a CLSM system. The original White and Amos design (White et al., 1987) utilized a pair of galvanometer mirrors (fast x and slow y), which scanned across the field of view in a raster pattern. There are several reasons why this design has endured, and is still present in most modern confocal systems. Galvanometer-driven mirrors are limited-motion DC motors controlled by a closed loop servo-mechanism, which generate positional control by rotating the mirror shaft. This provides a very precise movement, while allowing the mirror to rotate at speeds up to 1 kHz. Faster scan rates can be achieved by the process of bidirectional scanning, whereby the fast galvanometer scans in the forward and backward direction. As such a process detects half the detected lines backwards, care must be taken to correct for unsynchronized movements, which may otherwise result in acquisition errors (compare Fig. 3A and B). In CLSM, this translates to images which can be raster-scanned at levels far exceeding the diffraction limit, with most systems capable of rendering a 512 × 512 pixel image in under 1 second.

While galvo-based mirrors are still the highest-resolving scanners, several devices have been developed to increase the scanning speed and allow for video-rate (or higher) imaging of dynamic processes. One such device is the resonant scanner (Callamaras & Parker, 1999; Leybaert, de Meyer, Mabilde, & Sanderson, 2005), a galvo-mirror that oscillates in a sinusoidal manner at high frequencies (usually between 4 to 16 kHz). This is accomplished by collecting images in the forward and backward scan (i.e., odd lines left to right, even lines right to left), and decelerating the mirrors once they pass the central point of the scan thus eliminating the need to reset at the start of each line. This sinusoidal movement and bidirectional capture lead to a pixel clock distortion and a reversed image, which are corrected for on the fly by the acquisition software. The resonant scanner offers 30 to 420 Hz acquisition rates, dependent on the resolution of the capture. Among the limitations of this approach is that the resonant frequency is fixed, thus the pixel dwell time (see below) cannot be adjusted. Furthermore, resonant scanners are inherently noisier than traditional galvanometers, as their increased exposure frequency is also light-limiting (Fig. 3C).

Another means of rapidly modulating the light path within a confocal system has come in the form of acousto-optical (AO) devices. Such devices utilize acoustic waves to establish a homogenous gradient in a birefringent crystal (typically TeO_2 or $PbMoO_4$), thus acting like an optical grating to bend specific wavelengths passing through it. AO devices include AO deflectors, which allow for laser scanning, AO modulators, which attenuate laser intensity, and AO tunable filters, which allow for rapid switching of excitation lasers. As AO deflectors have no moveable parts, they allow for extremely rapid raster

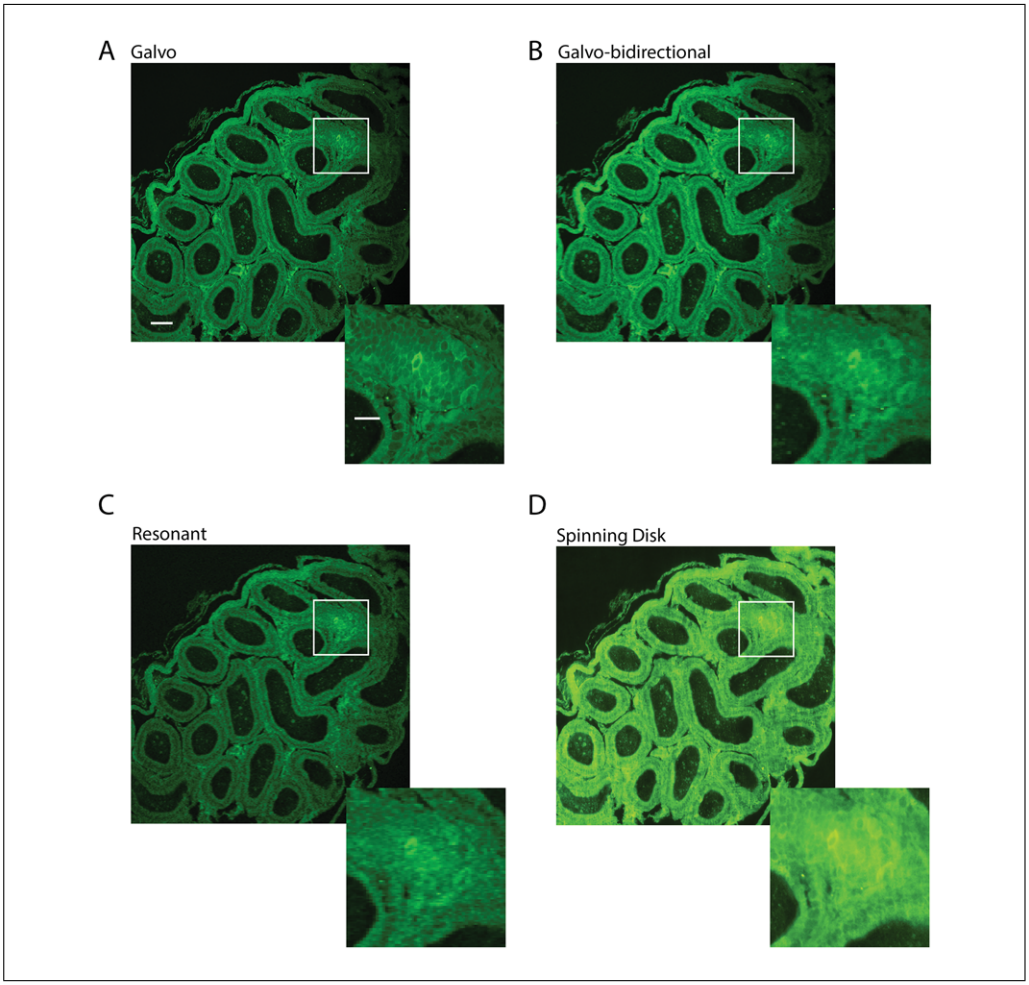

Figure 3 Comparison of different confocal imaging modalities. Acinus, imaged under unidirectional galvano-CLSM (**A**), uncorrected bidirectional galvano-CLSM (**B**), resonant scanner CLSM (**C**), and spinning disk confocal microscopy (**D**). Insets show the results of improper correction in bidirectional galvo scans, the reduced spatial resolution associated with resonant scanning, and the reduced z-axis resolution of the spinning disk confocal. Scale bars: 20 μm for whole FOV; 5 μm for inset.

scans, often exceeding 1 kHz (Chen, Leischner, Rochefort, Nelken, & Konnerth, 2011; Otsu et al., 2008). Limitations of AODs include a relatively small deflection angle (~1/3 of mirror-based deflectors) and marginally lower resolution resulting from laser beam dispersion (Römer & Bechtold, 2014).

Confocal Aperture

The ability to change the size of the confocal aperture allows optimal resolution images from samples with different fluorophores to be acquired. Over the past three decades, there have been several geometric changes to the shape of the pinhole, some of which have offered enhanced resolution or increased acquisition speeds. While the White and Amos design used a circular iris, a number of subsequent designs have employed square or hexagonal geometries for the confocal aperture. There are certainly arguments for using one geometry over another. Proponents of the hexagonal pinhole have suggested that such a design is a closer approximation of the "ideal" circular design, and allows 30% more light throughput, thus producing brighter images (Light & Maverick, 2008). This claim is somewhat dubious, as light throughput is defined by the area of a pinhole and is independent of shape. A square pinhole may, in fact, offer a resolution advantage

when utilized in systems using dispersive elements, such as spectral detectors, in part due to its rotational asymmetry (Engelhardt 1998).

Another fundamentally-different approach to the confocal aperture has utilized a vertical slit, rather than a pinhole. The principle behind this approach is to increase the vertical size of galvanometer sweeps, and thus increase the rates of acquisition. This approach has been in use along with acousto-optical devices, generating frame rates in excess of 100 Hz (Han, Im, Park, Kim, & Kim, 2005), or in combination with light sheet excitation to improve optical sectioning (Baumgart & Kubitscheck, 2012). Slit-confocal microscopy is limited by reduced resolution and optical sectioning abilities, when compared with point-scanning approaches.

Excitation Light Sources

CLSM systems utilize laser emission as a collimated light source to generate a diffraction-limited excitation spot at the focal plane of a sample. Traditionally, these lasers have been gas-based, with the two most prominent ones being the HeNe laser, with emission at the 633 nm (and later modified to the 543 nm) wavelength, and the Argon-ion with peak emissions at 488 nm and 514 nm. While some modern CLSM systems still employ Argon-ion lasers, they are increasingly making use of solid state and diode lasers, which offer greater stability, emit less heat, and have no requirements for cooling. Diode lasers, in particular, are an attractive option due to their compact size and fast modulation frequencies.

Most CLSM systems are designed to image multiple fluorophores, and as such, require the use of a number of separate laser lines to provide efficient excitation. Recent advances have aimed to resolve this issue by developing a single laser source which could generate various emission wavelengths. One such device uses a photonic crystal fiber (PCF) to generate a supercontinuum white light laser capable of emitting all colors between 460 nm and 2 μm in wavelength simultaneously. Through the use of narrow bandpass or acousto-optic tunable filters, it is possible to select a specific excitation wavelength.

Microscope

One of the attractive features of a CLSM system is that a scan head can be incorporated into virtually any upright or inverted fluorescent microscope frame. Such microscopes are typically outfitted with a range of high- numerical aperture objectives to maximize the resolving power of the system, and include an epifluorescent light source which allows for sample visualization and focusing. A piezo- driven motorized stage can provide automated multi-point recordings, and faster and more accurate axial movement in the generation of confocal z-stacks. Confocal systems designed for live-cell imaging typically include a chamber with controlled temperature, humidity, and gas exchange, which integrate into the microscope stage.

ALTERNATIVE CONFOCAL MICROSCOPES

While CLSM has become synonymous with ‘confocal microscope’, it is important to note that there have been alternative approaches to confocal microscopy. The most prominent of these is the spinning disk confocal approach, which has established itself as a viable and fast alternative to scanning confocal microscopy.

Spinning Disk Confocal

The spinning disk confocal (SDC) microscope utilizes a rotating disk with concentric circles of pinholes in the excitation beam path to generate a multiplex of excitation and detection spots, thus allowing for the rapid scanning of an entire field of view. The disk

was first conceptualized by Paul Nipkow in 1884 (Nipkow 1884), and consists of a series of pinholes arranged in an Archimedean spiral of constant pitch. As the disk is rotated, the apertures separate the image in a linear manner, thus allowing it to be transmitted and reconstructed. The Nipkow disk presents the first means of viewing images as electrical signals, and was the basis of the first mechanical television in 1926.

In the late 1960's the Nipkow disk was used as the basis of a new sectioning microscope by Egger and Petráň, which they dubbed the 'tandem scanning reflected light microscope' (Egger & Petran, 1967; Petran, Hadravsky, Egger, & Galambos, 1968). In this design, a disk consisting of ~1000 symmetrically-arranged, left- and right-hand interleaved pattern of pinholes was illuminated by an arc light, and the excitation was focused onto a sample. Reflected light from the specimen was then directed through the laterally-opposite side of the disk containing a diametrically-opposed set of pinholes, which served as a confocal aperture to reject out of focus light. A simplified version of the spinning disk confocal was designed in the late 1980's by Gordon Kino and Jeff Lichtman, in which they used the same pinholes to simultaneously illuminate samples and detect emitted light (Lichtman, Sunderland, & Wilkinson, 1989, Xiao, Corle, & Kino, 1987). In this permutation, the Nipkow disk was oriented at a slight angle to deflect the excitation light away from the optical axis. These initial versions of the spinning disk confocal offered significant gains in speed of acquisition, when compared with single-point scanning systems, while also offering resolutions and optical sectioning capabilities that were comparable to CLSM systems. Nonetheless, the introduction of the Nipkow disk in the optical path led to drastic attenuation of illumination, with most systems offering ~5% light throughput, thus making them unsuitable for anything but the brightest of samples (Amos & White, 2003).

In 1992, Yokogawa developed a spinning disk scan head design, which has become the gold standard for SDC systems. In this design, the excitation laser source is first focused on a disk containing 20,000 microlenses spinning at 4 to 10 kHz, which serves to focus the beam to the aligned apertures in the Nipkow disk. Emitted light passes back through the spinning disk, and is reflected to a dichroic mirror to a detector, typically a CCD or sCMOS camera (Fig. 4A). By using the microlens array, the Yokogawa scan head has been shown to increase illumination throughput by almost an order of magnitude (Tanaami et al., 2002).

The speed advantage of the SDC over point scanning systems, such as the CLSM, stems from the manner in which the imaging plane is illuminated and recorded from. As discussed above, a CLSM modulates the location of a laser excitation spot through a pair of galvanometer mirrors or AODs, and generates an image by scanning in a raster pattern across the field of view (Fg. 4B, top). In the SDC, points are scanned in parallel, in the form of concentric circles, generated as the disk rotates (Fig. 4B, bottom). The pinhole pattern on the Yokogawa Nipkow disk, for example, is designed to scan an entire image with a 30-degree rotation of the disk. With rotation frequencies in the kHz range, such a system is capable of sub-millisecond recordings.

There are several limitations of a spinning disk confocal system that are associated with its operation. Introduction of the spinning disk head within the path of acquisition will inherently block a portion of the field of view, requiring cropping of the final image. While this may not be a concern in terms of image resolution with most modern sCMOS cameras, it does pose limitations on the area of the sample that could be visualized at one time. Another shortcoming of the SDC as compared with CLSM systems is that the pinhole diameter is fixed. This results in sub-optimal axial resolution with some lenses (of lower numerical aperture), which, in turn, limits the sectioning capabilities of a spinning disk system (Fig. 3D). Unlike point scanning systems, which have the option

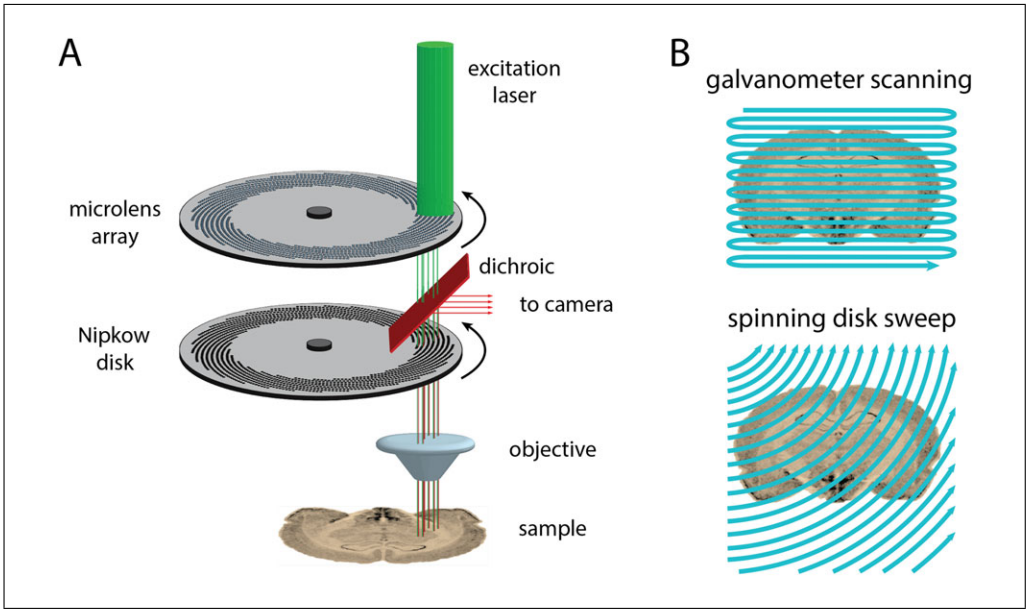

Figure 4 The spinning disk confocal. (**A**) A diagrammatic representation of a modern spinning disk confocal microscope. Laser excitation is delivered to the spinning disk unit through a fiber optic light guide, and is projected onto an array of microlenses. The separated beam then passes through a dichroic mirror and the aligned apertures of the spinning disk. Emitted signal passes back through the spinning disk, and is reflected off the dichroic to a CCD or CMOS camera. (**B**) Illumination approach in point scanning (top) and spinning disk (bottom) systems. The galvanometer scans are performed in a point by point manner, scanning across in a raster pattern. The spinning disk approach, on the other hand employs multiple site illumination and detection, sweeping across the FOV.

to use spectral array detectors, SDC microscopes require multiple cameras to perform simultaneous multiple- fluorophore recordings, which typically limits a spinning disk system to recording from two colors concurrently.

SDC microscopy has established itself as an indispensable approach for the study of dynamic biological processes. The inherent splitting of laser illumination, coupled with the short duration of exposure, results in a system which induces low bleaching and phototoxicity, thus making it particularly suitable for the study of living cells. In modern microscopy, the SDC is viewed as a method that works in tandem with, rather than serving as an alternative to, CLSM.

Swept Field Confocal

Another approach that utilizes multi-spot illumination and detection of fluorescent signals is the swept field confocal (SFC) microscope. Similar to the spinning disk approach, SFC projects the excitation laser onto a series of pinholes or slits, thus splitting the beam. Unlike SDC, this pinhole array is stationary, and the beam is swept across the sample through the use of galvanometer- and piezzo-controlled mirrors. Emitted light is descanned back by the mirrors, projected through a complimentary set of apertures on the pinhole array, and acquired by a fast camera. While initial implementations of the SFC plate used 2-dimensional arrays of pinholes, this unfortunately generated pinhole crosstalk, whereby adjacent signals interfered with one another, leading to a loss in resolution. Newer plates use a single column of 32 pinholes, which allow for rapid (up to 100 Hz) scanning across the field of view. An added advantage is that the SFC array plates include columns of apertures of different sizes (typically between 30 to 90 µm in diameter), allowing for optimized resolution contingent on sample and fluorophores used, as well as a set of slits, which allow imaging at rates exceeding 1000 Hz. Obtaining sufficient signals at such speeds requires bright illumination sources and detectors with

high sensitivities. To these ends, SFC systems typically employ higher power of excitation lasers (Castellano-Munoz, Peng, Salles, & Ricci, 2012) and cameras with larger pixel sizes.

The obvious advantages of an SFC system is the sheer speed of acquisition, enabling the detection of dynamic cellular processes. Acquisition rates are truly limited only by the CCD cameras used to detect emission. As of now, cameras with the ability to record in excess of 1000 Hz are resolution-limited, though this is a field of active development; cameras with improved resolution are likely to be available in the near future. The reduced temporal exposure to excitation light also reduces the probability of phototoxicity or bleaching of live specimens, which is advantageous when imaging more sensitive samples. Other limitations of SFC, when compared with CLSM, include reduced resolution and optical sectioning abilities, and lower dynamic range, due to the inherent disadvantages of using a CCD detector vs a PMT.

PRACTICAL CONSIDERATIONS

In the hopes of providing a starting point to the novice confocal microscopist, we have assembled a brief list of common practices and considerations when using a confocal laser scanning microscope. This section is not intended to be a comprehensive list, but rather a discussion of how the acquisition parameters in CLSM integrate, and how modulation of each can optimize acquired image quality.

Fluorophore Selection

The single most important factor in obtaining satisfactory image data with a confocal microscope is proper fluorescent staining of tissues. Contrary to conventional wisdom, the use of a CLSM will not improve weak fluorescent signals. Indeed, the opposite is true, as introducing the confocal pinhole drastically reduces the amount of emission light that reaches the detector.

Multiple- fluorophore staining should be planned in order to utilize the available laser lines of the CLSM system in use, and to avoid fluorophore crosstalk. Most modern confocal systems have at least four standard laser lines, with excitation at 405, 488, 561, and 633 nm, capable of exciting blue, green, red, and far-red fluorophores, respectively. The 488 nm line is typically an Argon-ion laser, which can be used to emit at 458 nm and 514 nm, thus allowing for the activation of cyan and yellow fluorescent proteins. Spectral unmixing may be required when using either of those proteins in conjunction with a green fluorescent protein, due to their overlapping emission spectra.

Image Size and Resolution

Most modern confocal scan heads offer acquisition of images upwards of 8192 pixels per edge in the x- and y-axes. While it is tempting to think that higher pixel densities yield images containing more spatial information, this is typically not the case. As mentioned earlier, the diffraction limit is defined by the wavelength of excitation and the numerical aperture of the lens used to image. Super-sampling beyond this point is time consuming, takes up storage resources, and does not yield any additional resolution. Most modern acquisition software can calculate the optimal lateral resolution based on the laser line and objective used.

Point scanning systems are inherently capable of scanning smaller regions of the FOV, thus creating a form of an optical zoom. Unlike digital zoom, which has a fixed pixel pitch, optically zooming does not degrade image resolution, and can readily be used up to 4× with high NA objectives (Fig. 5). This is a useful approach, as it allows visualization of smaller structures without having to change objectives.

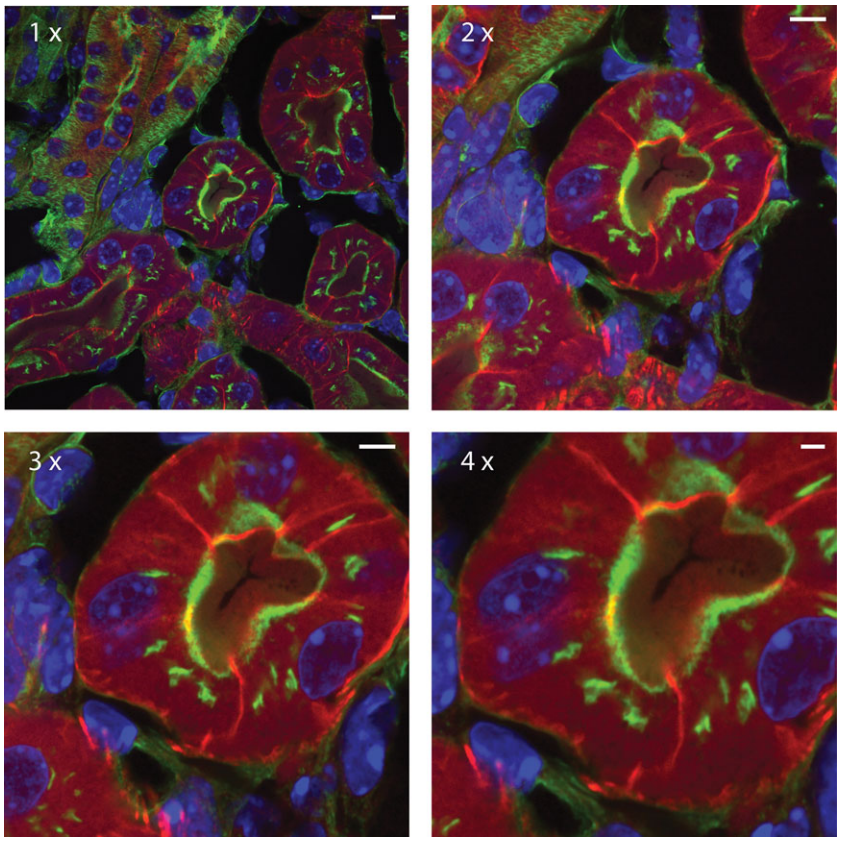

Figure 5 Optical magnification on a scanning confocal microscope. The images show the same field of view imaged at 1×, 2×, 3×, and 4×, showing the lens maintaining good resolution through the magnification range. Scale bars: 1×: 8 μm, 2×: 6 μm, 3×: 4 μm, 4×: 2 μm.

Triangle of Compromise

In confocal microscopy, as in all other microscopy approaches, there exists the notion of the triangle of compromise. There are three essential apexes in confocal microscopy-speed, sensitivity, and resolution, and in order to maximize one value, we must compromise on one or both of the other criteria. If, for example, the goal is to acquire images with the greatest speed possible, this can be achieved by either reducing the resolution of acquisition, or by suffering with lower detection sensitivity. Conversely, optimal resolution images typically require longer scans.

In using a CLSM system there are several parameters which the user can control to establish the priorities of their acquisitions. One such parameter is pixel dwell time, or the time that the laser scanning system spends on a single point (a value typically on the microsecond timescale). Increasing the pixel dwell time increases the number of photons which are collected by the PMT, increasing the detection sensitivity and dynamic range. Longer pixel dwell times will, however, increase the frame acquisition period, and hold a higher chance of photobleaching or phototoxicity. Modulating the amount of laser power used to excite a fluorophore is another parameter that the user typically controls. Increased laser intensity results in greater fluorophore excitation, producing images with higher dynamic range and contrast, but again may lead to photobleaching. The ability to control the PMT detector gain, allows for the detection of dimmer fluorescence, though care must be taken, as increased amplification can lead to elevated levels of shot noise and decrease dynamic range. Image balance can further be controlled by the size of the

confocal aperture. This size is typically expressed as a proportion of the Airy unit, and it differs for each excitation wavelength/lens NA combination. Increasing the size of the confocal pinhole will allow a greater number of photons to reach the detector, but this increase in sensitivity will reduce the resolution advantage gained by using a smaller pinhole.

Noise Reduction

Optimal microscopy images exhibit high dynamic range, low noise, and high levels of contrast. The majority of noise in acquisition typically results from weak signal to noise ratios, and the subsequent use of high PMT gains to increase detection sensitivity. There are several parameters to consider in order to reduce this noise. One is the pixel dwell time, which, as discussed earlier, will increase the system sensitivity and dynamic range at the cost of speed and potential for photobleaching. Another approach is to perform multiple acquisitions and either average them together in order to reduce PMT shot noise, or to sum the signals to improve the signal to noise ratio. Averaging, however, requires significantly longer acquisition periods, and can induce photobleaching as well as reduce image sharpness due to minute system movements.

Multi-Dimensional Acquisition

One of the most attractive features of CLSM as a technique is the capability to record optical sections and to subsequently reconstruct them into a three-dimensional object. Such z-stacks are typically performed from 'black to black', where the initial sections are captured at regions above the sample being imaged, and are performed through to the other end of the sample. This is done to ensure the entire volume of the image would be captured. Another acquisition approach allows the user to select a central point, and make optical sections at a pre-determined depth above and below that point. The step size of such optical sections is of paramount importance, as large z-steps will lead to poor volume rendering. As discussed above, the z-axis resolution is a function of the numerical aperture of the objective, the emission wavelength, and the confocal aperture. Optimal z-step size is determined by the Nyquist sampling theorem, which states that the sampling frequency should be at least twice the z-axis resolution in order to avoid aliasing. From a practical perspective, it is imperative to avoid either under-sampling, which will prevent the capture of sufficient information for reconstruction, or oversampling, which does not generate any additional information, is time consuming, and can lead to sample bleaching. Most modern acquisition software will calculate Nyquist step size automatically, though it is important to optimize the acquisition per sample.

There are also several considerations that must be accounted for when performing multiple fluorophore imaging. Modern confocal systems offer the option to record different fluorescence channels by either switching the excitation every line or every frame. Switching excitation per line offers faster image acquisition rates, as the slower (y-axis) galvanometer has to scan the field of view only once. The drawback to this approach is that when switching every line, most CLSM systems will keep the confocal aperture constant, typically for the fluorophore with the longest wavelength. Doing so may not generate the optimal resolution at shorter wavelengths, and when optimal resolution is desired, channel switching should be performed per frame.

CONCLUSION

In this chapter, we have attempted to consolidate the development, principles, and practical considerations of confocal laser scanning microscopy. New technologies continue to push the possibilities of what confocal microscopy can offer even further, with integration of sub-diffraction limited imaging modalities and faster scanning abilities. Already

a cornerstone for most biological optical studies, CLSM is likely to remain so for the foreseeable future.

ACKNOWLEDGEMENTS

We gratefully acknowledge support from Washington University School of Medicine, The Children's Discovery Institute of Washington University, and St. Louis Children's Hospital under grant number CDI-CORE-2015-50 and the Foundation for Barnes-Jewish Hospital under grant number 3770. Confocal laser scanning microscopy data shown was generated by a Zeiss LSM 880 Airyscan Confocal Microscope, which was purchased with support from the Office of Research Infrastructure Programs (ORIP), a part of the NIH Office of the Director, under grant number OD021629.

LITERATURE CITED

Amos, W. B., & White, J. G. (2003). How the confocal laser scanning microscope entered biological research. *Biologie Cellulaire*, *95*(6), 335–342. doi: 10.1016/S0248-4900(03)00078-9.

Amos, W. B., White, J. G., & Fordham, M. (1987). Use of confocal imaging in the study of biological structures. *Applied Optics*, *26*(16), 3239–3243. doi: 10.1364/AO.26.003239.

Axelrod, D. (1981). Cell-substrate contacts illuminated by total internal reflection fluorescence. *Journal of Cell Biology*, *89*(1), 141–145. doi: 10.1083/jcb.89.1.141.

Baumgart, E., & Kubitscheck, U. (2012). Scanned light sheet microscopy with confocal slit detection. *Optics Express*, *20*(19), 21805–21814. doi: 10.1364/OE.20.021805.

Brakenhoff, G. J., Blom, P., & Barends, P. (1979). Confocal scanning light microscopy with high aperture lenses. *Journal of Microscopy*, *117*, 219–232. doi: 10.1111/j.1365-2818.1979.tb01178.x.

Brakenhoff, G. J., van Spronsen, E. A., van der Voort, H. T., & Nanninga, N. (1989). Three-dimensional confocal fluorescence microscopy. *Methods in Cell Biology*, *30*, 379–398. doi: 10.1016/S0091-679X(08)60987-5.

Bridges, W. B. (1964). Laser oscillation in singly ionized Argon in the visible spectrum. *Applied Physics Letters*, *4*(7), 128–130. doi: 10.1063/1.1753995.

Callamaras, N., & Parker, I. (1999). Construction of a confocal microscope for real-time x-y and x-z imaging. *Cell Calcium*, *26*(6), 271–279. doi: 10.1054/ceca.1999.0085.

Castellano-Munoz, M., Peng, A. W., Salles, F. T., & Ricci, A. J. (2012). Swept field laser confocal microscopy for enhanced spatial and temporal resolution in live-cell imaging. *Microscopy and Microanalysis*, *18*(4), 753–760. doi: 10.1017/S1431927612000542.

Chen, X., Leischner, U., Rochefort, N. L., Nelken, I., & Konnerth, A. (2011). Functional mapping of single spines in cortical neurons in vivo. *Nature*, *475*(7357), 501–505. doi: 10.1038/nature10193.

Cole, R. W., Thibault, M., Bayles, C. J., Eason, B., Girard, A. M., Jinadasa, T., ... Brown, C. M. (2013). International test results for objective lens quality, resolution, spectral accuracy and spectral separation for confocal laser scanning microscopes. *Microscopy and Microanalysis*, *19*(6), 1653–1668. doi: 10.1017/S1431927613013470.

Davidovits, P., & Egger, M. D. (1969). Scanning laser microscope. *Nature*, *223*(5208), 831. doi: 10.1038/223831a0.

Denk, W., Strickler, J. H., & Webb, W. W. (1990). Two-photon laser scanning fluorescence microscopy. *Science*, *248*(4951), 73–76. doi: 10.1126/science.2321027.

Dickinson, M. E., Bearman, G., Tille, S., Lansford, R., & Fraser, S. E. (2001). Multi-spectral imaging and linear unmixing add a whole new dimension to laser scanning fluorescence microscopy. *Biotechniques*, *31*(6). *1272*, 1274–1276, 1278.

Dunn, K. W., Kamocka, M. M., & McDonald, J. H. (2011). A practical guide to evaluating colocalization in biological microscopy. *American Journal of Physiology. Cell Physiology*, *300*(4), C723–742. doi: 10.1152/ajpcell.00462.2010.

Egger, M. D., & Petran, M. (1967). New reflected light microscope for viewing unstained brain and ganglion cells. *Science*, *157*, 305–307. doi: 10.1126/science.157.3786.305.

Engelhardt, J. (1998). *Optical arrangement provided for a spectral fanning out of a light beam*. USA. 6801359 B1.

Erhardt, A., Zinser, G., Komitowski, D., & Bille, J. (1985). Reconstructing 3-D light-microscopic images by digital image processing. *Applied Optics*, *24*(2), 194. doi: 10.1364/AO.24.000194.

Han, S., Im, K. B., Park, H., Kim, D., & Kim, B. M. (2005). *High Speed Slit-Scanning Confocal Laser Microscopy with an Acousto- Optic Beam Deflector and a Line Scan Camera*. San Jose, CA: SPIE BiOS.

Haraguchi, T., Shimi, T., Koujin, T., Hashiguchi, N., & Hiraoka, Y. (2002). Spectral imaging fluorescence microscopy. *Genes to Cells*, *7*(9), 881–887. doi: 10.1046/j.1365-2443.2002.00575.x.

Julius, M. H., Masuda, T., & Herzenberg, L. A. (1972). Demonstration that antigen-binding cells are precursors of antibody-producing cells after purification with a fluorescence-activated cell sorter. *Proceedings of the National Academy of Sciences of the United States of America*, *69*(7), 1934–1938. doi: 10.1073/pnas.69.7.1934.

Lazarides, E., & Weber, K. (1974). Actin antibody: The specific visualization of actin filaments in non-muscle cells. *Proceedings of the National Academy of Sciences of the United States of America*, *71*(6), 2268–2272. doi: 10.1073/pnas.71.6.2268.

Leybaert, L., de Meyer, A., Mabilde, C., & Sanderson, M. J. (2005). A simple and practical method to acquire geometrically correct images with resonant scanning-based line scanning in a custom-built video-rate laser scanning microscope. *Journal of Microscopy*, *219*(Pt 3), 133–140. doi: 10.1111/j.1365-2818.2005.01502.x.

Lichtman, J. W., Sunderland, W. J., & Wilkinson, R. S. (1989). High-resolution imaging of synaptic structure with a simple confocal microscope. *The New Biologist*, *1*(1), 75–82.

Light, V. J., & Maverick, G. (2008). Paradigm shift in laser scanning confocal microscopy: Resonant real time live spectral imaging for cell dynamics. *Journal of Advanced Biotechnology*, 36–40.

Maiman, T. H. (1960). Stimulated optical radiation in ruby. *Nature*, *187*, 493–494. doi: 10.1038/187493a0.

Minsky, M. (1957). Microscopy Apparatus. Pat. No. 3013467. United States.

Minsky, M. (1988). Memoir on inventing the confocal scanning microscope. *Scanning*, *10*, 128–138. doi: 10.1002/sca.4950100403.

Neil, M. A., Juskaitis, R., & Wilson, T. (1997). Method of obtaining optical sectioning by using structured light in a conventional microscope. *Optics Letters*, *22*(24), 1905–1907. doi: 10.1364/OL.22.001905.

Nipkow, P. (1884). Electric telescope. G. E. (Berlin). Germany.

Osborne, M. A., Balasubramanian, S., Furey, W. S., & Klenerman, D. (1998). Optically biased diffusion of single molecules studied by confocal fluorescence microscopy. *The Journal of Physical Chemistry*, *102*, 3160–3167. doi: 10.1021/jp9715078.

Otsu, Y., Bormuth, V., Wong, J., Mathieu, B., Dugue, G. P., Feltz, A., & Dieudonne, S. (2008). Optical monitoring of neuronal activity at high frame rate with a digital random-access multiphoton (RAMP) microscope. *Journal of Neuroscience Methods*, *173*(2), 259–270. doi: 10.1016/j.jneumeth.2008.06.015.

Pawley, J. B. (2006). *Handbook of biological confocal microscopy*. New York: NY, Springer.

Petran, M., Hadravsky, M., Egger, M. D., & Galambos, R. (1968). Tandem scanning reflected light microscope. *Journal of the Optical Society of America*, *58*, 661–664. doi: 10.1364/JOSA.58.000661.

Roe, M. W., Fiekers, J. F., Philipson, L. H., & Bindokas, V. P. (2006). Visualizing calcium signaling in cells by digitized wide-field and confocal fluorescent microscopy. *Methods in Molecular Biology*, *319*, 37–66. doi: 10.1007/978-1-59259-993-6_3.

Römer, G. R. B. E., & Bechtold, P. (2014). Electro-optic and acousto-optic laser beam scanners. *Physics Procedia*, *56*, 29–39. doi: 10.1016/j.phpro.2014.08.092.

Scheenen, W., & Carmignoto, G. (2002). *Confocal Imaging of Calcium Signaling in Cells from Acute Brain Slices*. New York: NY, Springer.

Sekar, R. B., & Periasamy, A. (2003). Fluorescence resonance energy transfer (FRET) microscopy imaging of live cell protein localizations. *Journal of Cell Biology*, *160*(5), 629–633. doi: 10.1083/jcb.200210140.

Stokes, T. (2005). Tutorial: Avalanche Photodiodes Theory And Applications.

Tanaami, T., Otsuki, S., Tomosada, N., Kosugi, Y., Shimizu, M., & Ishida, H. (2002). High-speed 1-frame/ms scanning confocal microscope with a microlens and Nipkow disks. *Applied Optics*, *41*(22), 4704–4708. doi: 10.1364/AO.41.004704.

Vukojevic, V., Heidkamp, M., Ming, Y., Johansson, B., Terenius, L., & Rigler, R. (2008). Quantitative single-molecule imaging by confocal laser scanning microscopy. *Proceedings of the National Academy of Sciences of the United States of America*, *105*(47), 18176–18181. doi: 10.1073/pnas.0809250105.

Wallén, P., Di Prisco, G., & Dubuc, R. (1991). Investigating the Three-Dimensional Morphology of Fluorescence-Labelled Neurons Using Confocal Laser Scanning Microscopy. *Neurocytochemical Methods. NATO ASI Series (Series H: Cell Biology)*. A. Calas and E. D. Berlin, Springer. *58*.

White, A. D., & Ridgen, J. D. (1962). Continuous gas maser operation in the visible. *Proceedings of the IRE*, *50*, 1697.

White, J. G., & Amos, W. B. (1987). Confocal microscopy comes of age. *Nature*, *328*, 183–184. doi: 10.1038/328183a0.

White, J. G., Amos, W. B., & Fordham, M. (1987). An evaluation of confocal versus conventional imaging of biological structures by fluorescence light microscopy. *Journal of Cell Biology*, *105*(1), 41–48. doi: 10.1083/jcb.105.1.41.

Wilson, T. (2011). Optical sectioning in fluorescence microscopy. *Journal of Microscopy*, *242*(2), 111–116. doi: 10.1111/j.1365-2818.2010.03457.x.

Wilson, T. (2011). Resolution and optical sectioning in the confocal microscope. *Journal of Microscopy*, *244*(2), 113–121. doi: 10.1111/j.1365-2818.2011.03549.x.

Xiao, G. Q., Corle, T. R., & Kino, G. S. (1987). A real-time confocal scanning optical microscope. *Applied Physics Letters*, *53*, 716–718. doi: 10.1063/1.99814.

Young, J. Z., & Roberts, F. (1951). A flying spot microscope. *Nature*, *167*(4241), 231. doi: 10.1038/167231a0.

Zipfel, W. R., Williams, R. M., & Webb, W. W. (2003). Nonlinear magic: Multiphoton microscopy in the biosciences. *Nature Biotechnology*, *21*(11), 1369–1377. doi: 10.1038/nbt899.